RASĀYAN *J. Chem.*
Vol. 19 | No. 3 | 1683-1691 | July-September | 2026
ISSN: 0974-1496 | e-ISSN: 0976-0083 | CODEN: RJCABP
http://www.rasayanjournal.com
http://www.rasayanjournal.co.in

ADVANCED POLY(MELAMINE)/GOLD NANOPARTICLE-MODIFIED CARBON PASTE ELECTRODE FOR SIMULTANEOUS DETECTION OF URIC ACID AND DOPAMINE IN URINE

E.Fitriany[1,3], M. Harsini[2,✉], F. Kurniawan[1], B. A. Widyaningrum[4], and D. R. A. Paramita[5]

[1]Department of Chemistry, Institut Teknologi Sepuluh Nopember, Surabaya, 60111, Indonesia
[2]Department of Chemistry, Universitas Airlangga, Surabaya, 60115, Indonesia
[3]Department of Analytical Chemistry, Akademi Farmasi Mitra Sehat Mandiri Sidoarjo, Sidoarjo, 61262, Indonesia
[4]Research Center for Biomass and Bioproducts, National Research and Innovation Agency (BRIN), Bogor 16911, Indonesia
[5]Department of Pharmacy, Akademi Farmasi Jember, Jember, 68125, Indonesia
✉Corresponding author: muji-h@fst.unair.ac.id

ABSTRACT

A novel electrode modification strategy was developed. It involved electropolymerization of melamine and electrodeposition of gold nanoparticles (AuNPs) onto a carbon paste electrode (CPE), forming a polymelamine (PM)/AuNPs-modified electrode. The fabricated AuNPs/PM/CPE electrode was designed for the simultaneous determination of uric acid (UA) and dopamine (DA). Field Emission Scanning Electron Microscopy-Energy Dispersive X-ray analysis (FESEM-EDX) revealed that the AuNPs/PM/CPE electrode exhibited a surface morphology with a large effective area, facilitating enhanced electrochemical activity for the simultaneous detection of both compounds in human urine samples. Optimisation studies determined that a scan rate of 100 mV/s was optimal. A 0.1 M phosphate-buffered saline (PBS, pH 3.0) solution was selected as the supporting electrolyte for simultaneous determination. The LoD values for DA and UA were 0.6052 µM and 0.6462 µM, respectively, with high correlation coefficients (R^2 = 0.9981 for DA and 0.9979 for UA). The sensor showed strong analytical performance, with recoveries of 89.6–109.2% for DA and 83.4–105.1% for UA. Precision values ranged from 0.02–0.70% for DA and 0.06–0.63% for UA. The standard-addition (spiking) method applied to human urine yielded recoveries of 98.99% for DA and 98.96% for UA at a concentration of 1 µM. The developed sensor provides a rapid, cost-effective, and minimally invasive approach for monitoring DA and UA in urine, offering considerable potential for early diagnosis and clinical screening of neurological and metabolic disorders. Its superior analytical performance is attributed to the uniform dispersion of AuNPs, which enhances electron transfer efficiency and catalytic responsiveness.

Keywords: Gold nanoparticles, Polymelamine, Uric acid, Dopamine, Electrochemical sensor.

INTRODUCTION

Uric acid (UA) and dopamine (DA) are key components of human metabolism and physiological regulation. Both also serve as important biomarkers for various health conditions**.** UA represents the final product of purine metabolism. Its serum levels usually range from 0.13 to 0.46 mM.[1] Accurate monitoring is important because elevated UA levels indicate hyperuricemia, which is a major diagnostic marker for kidney and metabolic disorders. DA is a neurotransmitter produced in the brain. It helps regulate motor function, mood, and other neurological processes. DA levels are also linked to cardiac function, blood pressure, and blood flow.[2] In healthy people, 24-hour urinary DA excretion ranges from 65 to 400 µg.[3] Low DA levels can widen blood vessels in the kidneys and heart, thereby increasing blood flow. High DA levels may result in elevated blood pressure. Abnormal DA levels are associated with neurological

http://doi.org/10.31788/RJC.2026.1929663

disorders, including Parkinson's disease, Alzheimer's disease, and depression.[4] Because of these links, research on DA and UA detection tools for early diagnosis has increased. Biosensors, in particular**,** have become effective for continuous, non-invasive biomarker monitoring, thereby facilitating early disease detection in healthcare. However, many studies on the detection of DA or UA in urine are challenged by environmental factors and varying analyte concentrations. These issues reduce the reliability of measurements under practical conditions.[5] Electrochemical studies on the simultaneous detection of UA and DA are still scarce. Existing sensors often cannot provide both a wide linear detection range and high sensitivity.[6] In addition**,** only a limited number of these sensors have been tested using real human samples. These limitations highlight the need for electrochemical sensors capable of simultaneously detecting both biomarkers with high analytical performance for clinical applications. This study aims to develop an electrochemical sensor with high sensitivity, selectivity, and reliability for the simultaneous detection of both compounds in human urine. This need is driven by current technological limitations, as only a few platforms combine high sensitivity, a wide linear detection range, and stable, reproducible performance in real human samples. Furthermore, additional clinical validation is required. To address these challenges, polymelamine (PM) and gold nanoparticles (AuNPs) were combined to improve the electrode's performance through their synergistic effects, thereby enhancing analytical efficiency and practical applicability. We report the fabrication and evaluation of an AuNPs/PM/CPE-modified carbon paste electrode for the sensitive and selective simultaneous detection of DA and UA. The combined effects of PM and AuNPs enhance the electrochemical performance, selectivity, and sensitivity of carbon paste electrodes (CPE). We used FESEM-EDX to examine the electrode's surface morphology and material distribution. Both DPV and CV were used to investigate the electrochemical behaviour of UA and DA. These methods were employed to establish the optimal experimental conditions and evaluate key analytical parameters, including linearity, sensitivity, detection limit, and selectivity. Previous work reported a sensor for DA and AA.[7] The current study extends this research. The practical applicability of the modified electrode was validated using urine samples, confirming its potential for clinical and diagnostic sensing. The development of this electrode aligns with Sustainable Development Goal (SDG) 3: Good Health and Well-Being**,** as it provides a promising platform for the early detection of diseases associated with abnormal DA and UA levels, thereby supporting improved healthcare outcomes**.**

EXPERIMENTAL

Apparatus and Reagents

Disodium hydrogen phosphate anhydrous (Na_2HPO_4), dopamine ($C_8H_{11}NO_2$), trisodium phosphate (Na_3PO_4), and sodium dihydrogen phosphate monohydrate ($NaH_2PO_4{\cdot}H2O$) were obtained from Sigma-Aldrich (USA). Ascorbic acid ($C_6H_8O_6$), phosphoric acid (H_3PO_4), hydrochloric acid (HCl), uric acid ($C_5H_4N_4O_3$), and urea (CH_4N_2O) were sourced from PT Smart Lab Indonesia. Ultra-high-purity water was provided by PT Brataco, Indonesia. An Autolab PGSTAT 128N potentiostat/galvanostat electrochemical workstation was used for all electrochemical studies, including differential pulse voltammetry (DPV) and cyclic voltammetry (CV). An Ag/AgCl (3M KCl) reference electrode, a Pt counter electrode, and a modified working electrode were used for the measurements. Surface morphology characterization was performed using a Hitachi SU 8220 field emission scanning electron microscope equipped with energy-dispersive X-ray spectroscopy (FESEM-EDX) at the Chemistry Laboratory, Institut Teknologi Sepuluh Nopember (ITS), Surabaya, Indonesia.

Fabrication of AuNPs/PM/CPE

The synthesis of the proposed AuNPs/PM/CPE electrode followed the fabrication procedure reported in our previous study[8] as shown in Fig.-1(a)First, we prepared the CPE by homogeneously mixing carbon powder and paraffin oil in a 7:3 (w/w) ratio. The resulting paste was packed into an electrode holder, and the surface was gently polished to achieve a uniform finish. The CPE surface was activated using cyclic voltammetry (CV) in 0.5 M H_2SO_4 at a scan rate of 100 mV/s for 30 cycles over a potential range of **0.0 to +1.0 V**, followed by rinsing with UHP water. Next, electropolymerization of melamine was performed on the activated CPE in 0.1 M NaOH containing 1 mM melamine at a scan rate of 100 mV/s for 20 cycles over a potential window of –0.1 to +1.6 V. AuNPs were electrodeposited onto the PM-modified CPE by

cyclic voltammetry in a mixed solution of 0.01M Na_2SO_4 and 0.01 M H_2 SO_4 containing 1 mM $HAuCl_4$ at a scan rate of 50 mV/s for 12 cycles over a potential range of –0.4 to +1.5 V. The modified electrodes were rinsed with UHP water and stored under dry conditions until use.

Electrochemical Measurements

Electrochemical measurements were performed in 0.1 M phosphate-buffered saline (PBS, pH 3.0) as the supporting electrolyte**.** The potential range applied in this study was +0.1 to +0.7 V to observe the electrochemical response of a mixed solution containing 100 µM UA and 100 µM DA. The scan rate was optimised using cyclic voltammetry (CV).

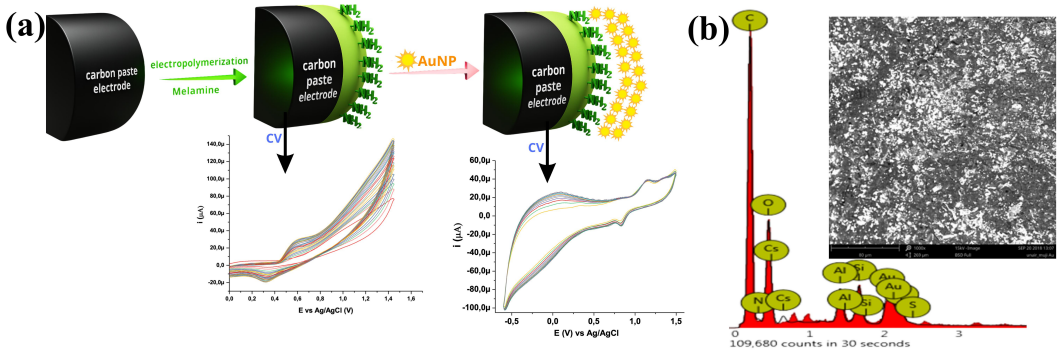

Fig.-1: (a) Schematic Fabrication Process of AuNPs/PM/CPE. (b) FESEM-EDX of AuNPs/PM/CPE

The scan rate variations investigated in this study were 20, 45, 60, 80, 100, 150, and 200 mV s^{-1}. The limit of detection (LoD) was determined from the calibration curves of UA and DA. The concentrations of UA and DA were varied over the range of 0.1–11 µM, while the concentration of the other analyte was kept constant. The LoD was calculated using the equation LoD = (3 × SD)/m.

Potential interference during the simultaneous detection of UA and DA in urine was evaluated by investigating the effects of relevant coexisting species, including ascorbic acid (AA), UA, and DA. Furthermore, reproducibility and repeatability tests were conducted to ensure the consistency and reliability of the analytical results obtained under different experimental conditions. These tests also evaluated the effects of sample matrix variation and the stability of the electrochemical response during repeated measurements.

Real Sample Analysis

The analytical performance, validity, and practical application of the modified AuNPs/PM/CPE electrode were assessed using newborn urine samples spiked with known concentrations of UA and DA. Newborn urine, with its simpler matrix and minimal interference, provides an optimal medium for method validation[9]. This matrix also provides a physiological baseline for studies involving DA and UA biomarkers, making it a safe, ethical, and efficient option for evaluating the selectivity of electrochemical sensors. To minimize matrix effects, urine samples were diluted 50-fold with 0.1 M PBS (pH 3.0) and centrifuged at 7000 rpm for 5 min**.** UA and DA at predetermined concentrations were then added to the samples, which were subsequently analyzed electrochemically using the modified working electrode.

RESULTS AND DISCUSSION

Material Characterization

The morphological characteristics of the AuNPs/PM/CPE electrode were comprehensively analyzed using FESEM-EDX. The resulting micrographs showed a relatively homogeneous distribution of gold particles on the electrode surface and provided elemental composition information, confirming the successful, significant, and consistent material modification. The electrode was composed of Au, C, O, N, and Si **(**Fig.-1(b)). Nitrogen detected in the EDX spectrum confirmed the successful electropolymerization of PM on the CPE surface. The PM coating prevented Au nanoparticles from aggregating into bulk gold.[10,11] The average size of the gold nanoparticles**,** determined using ImageJ, was 46.8 nm. FESEM revealed a homogeneous distribution of AuNPs with no visible aggregation. EDX showed that N was present at a

lower percentage than Au because the PM layer was covered by AuNPs. These findings demonstrate that PM serves as an effective substrate for AuNP immobilization, improving the surface properties of the modified electrode for the simultaneous detection of DA and UA. Furthermore, the hydrophilic nature of PM enhances the compatibility between AuNPs and the carbon-based electrode matrix.[12] The uniform distribution of AuNPs also increases the active surface area and the number of catalytic sites[13–15], thereby enhancing the electrochemical performance of the modified electrode for the simultaneous detection of DA and UA.

Electroanalytical Studies of AuNPs/PM/CPE

The electrochemical performance of UA and DA was evaluated using four types of working electrodes: AuNPs/PM/CPE, PM/CPE, AuNPs/CPE, and CPE, as shown in Fig.-2(a). This evaluation was conducted systematically to determine the optimal working electrode for the simultaneous detection of both analytes. Simultaneous measurements of UA and DA were performed using cyclic voltammetry (CV) over a potential range of −0.4 to +0.8 V at a scan rate of 100 mV/s. The voltammograms indicated that the bare CPE exhibited the lowest peak current (Ip), reflecting slow electron transfer at its surface. The PM/CPE demonstrated a higher Ip than the bare CPE, which was attributed to the amine functional groups and aromatic rings in polymelamine, facilitating molecular interactions and accelerating electron transfer. The AuNPs/CPE displayed pronounced anodic and cathodic currents, indicating enhanced electrochemical reversibility and improved electron-transfer kinetics, consistent with the high conductivity of gold nanoparticles. The developed AuNPs/PM/CPE electrode exhibited superior electrochemical characteristics, with clearly separated and well-defined oxidation peaks for UA and DA, enabling more selective and accurate simultaneous analysis. This enhanced resolution demonstrated the synergistic electrocatalytic effect of polymelamine and gold nanoparticles, resulting in improved sensor sensitivity and selectivity. In contrast, the AuNPs/CPE electrode alone did not achieve complete peak separation. These results demonstrated significant catalytic enhancement and a reduction in oxidation potential achieved through the dual-modification strategy, making the developed working electrode a promising platform for the simultaneous electrochemical detection of UA and DA. The nitrogen-rich structure and aromatic rings of polymelamine facilitate efficient electron transfer[16–18], supporting rapid and stable electron flow. Gold nanoparticles also accelerate reaction kinetic[19,20], enabling the amine groups of polymelamine to interact with both AuNPs and the target analytes, thereby increasing their accumulation on the AuNPs/PM/CPE surface. Polymelamine also stabilises the dispersion of AuNPs and minimises their oxidation and agglomeration. The results of this study demonstrate that the dual modification strategy using polymelamine and gold nanoparticles significantly enhances the sensor's sensitivity, selectivity, and catalytic activity for the simultaneous detection of UA and DA.

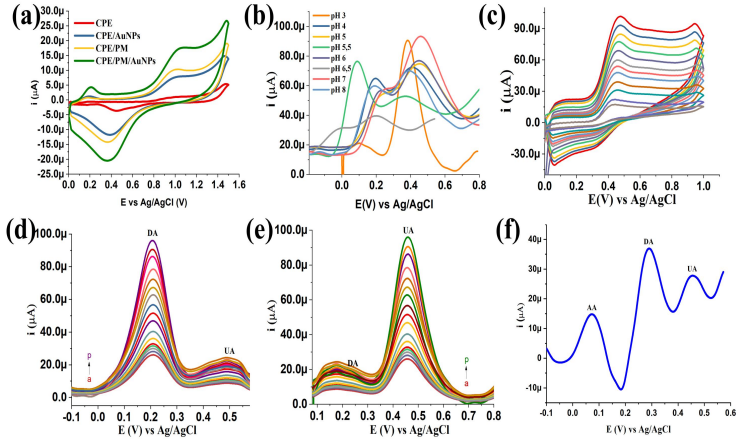

Fig.-2. (a) Electrochemical responses of different working electrodes toward the simultaneous detection of DA and UA; (b) Effect of pH; (c) Effect of scan rate; (d) DPV responses for DA at different concentrations; (e) DPV responses for UA at different concentrations; (f) Selectivity study in the presence of AA, DA, and UA.

The Effect of Supporting Electrolyte Measurement

The pH was optimized for electrochemical analysis to obtain maximum current responses with well-separated oxidation peaks. A 0.1 M phosphate-buffered saline (PBS) solution with pH values ranging from 3.0 to 9.0 was used to evaluate the effect of pH on the electrochemical behaviour of DA and UA. DPV measurements were conducted at a scan rate of 100 mV/s over an applied potential range of −0.18 to +0.8 V. The concentrations of DA and UA were maintained at 1 μM and 3 μM, respectively, throughout the optimization process to ensure that the observed current changes were solely attributed to variations in the pH of the supporting electrolyte.

Voltammograms recorded at pH 4.0, 5.0, 6.0, 6.5, 7.0, 8.0, and 9.0 (Fig.-2(b)) did not show satisfactory results due to the overlapping oxidation potentials of DA and UA under neutral and alkaline conditions. In contrast, clear separation of the UA and DA oxidation peaks was observed at pH 3.0 and 5.5, with the most distinct separation obtained at pH 3.0. At lower pH values, DA and UA are predominantly protonated, thereby minimizing intermolecular interactions and reducing peak broadening. Additionally, electron-transfer kinetics are enhanced under acidic conditions, resulting in sharper oxidation peaks and higher current responses. UA undergoes electrochemical oxidation through a proton-coupled electron-transfer process, forming urate-4,5-diol under appropriate electrochemical conditions[21,22]. Therefore, pH 3.0 was selected as the optimum supporting electrolyte condition for the simultaneous electrochemical detection of DA and UA.

The Effect of Scan Rate

Scan rate optimisation was performed to characterise electron-transfer kinetics, determine the most sensitive and stable measurement conditions, and clarify the reaction mechanism at the electrode surface[1,23].

This approach also enabled the evaluation of the redox behaviour of DA and UA, which was influenced by diffusion- or adsorption-controlled processes. Electrochemical measurements were performed by varying the scan rate from 20 to 450 mV s^{-1} to evaluate the kinetics and reaction mechanisms at the electrode surface. This variation allowed a comprehensive evaluation of the resulting current responses. The influence of scan rate was examined using cyclic voltammetry (CV). As illustrated in Fig.-2(c), increasing the scan rate resulted in higher anodic peak currents (Ipa) and a shift of the oxidation peak potential toward more positive values. These findings indicate that the electrochemical response is highly dependent on the scan rate. The relationship between log Ipa and log $v^{1/2}$ was linear, as demonstrated by the calibration plot ($Ipa = 0.456x + 0.5224$, $R^2 = 0.9784$). The oxidation process of UA and DA on the AuNPs/PM/CPE electrode followed a diffusion-controlled mechanism. The resulting peak current was strongly influenced by the mass-transfer rate of both analytes **to** the AuNPs/PM/CPE electrode surface. These results indicate that the electrochemical oxidation of UA and DA was governed predominantly by diffusion in solution rather than by the electron-transfer kinetics at the electrode surface, demonstrating that the overall process was diffusion-controlled.

Simultaneous Electrochemical Detection of UA and DA at AuNPs/PM/CPE

The performance and reliability of a sensor in detecting analytes at very low concentrations depend on the sensitivity of the working electrode. Sensitivity is a critical parameter for advancing modern biosensors and precision diagnostic systems[24]. The oxidation of both UA and DA on the AuNPs/PM/CPE electrode follows a diffusion-controlled mechanism, which is characteristic of homogeneous electrochemical systems. This behaviour indicates that the electrochemical reaction is predominantly governed by the diffusion of analytes from the bulk solution to the electrode surface, as supported by the linear relationship between the peak current and the square root of the scan rate, consistent with the Randles–Ševčík equation[25,26]. The generated current mainly depends on the rate of analyte mass transfer to the AuNPs/PM/CPE electrode surface. Accordingly, the electrochemical response is governed primarily by the availability of UA and DA at the electrode surface rather than by the kinetics of electron transfer. Consequently, increases in analyte concentration or the diffusion gradient lead directly to higher oxidation currents, confirming that the electrochemical process is predominantly diffusion-controlled. When the concentration of UA was fixed at 1 μM, the concentration of DA was gradually increased, resulting in a

proportional increase in the DA peak current. This result indicates a selective and sensitive electrode response to changes in DA concentration. In contrast, the UA peak current did not change significantly, indicating that increasing the DA concentration did not significantly interfere with the UA signal. This confirms the method's ability to perform accurate simultaneous detection with minimal mutual interference between the analytes. Conversely, the UA signal increased linearly with its concentration while the DA concentration was held constant at 1 μM, further confirming the sensor's high selectivity. The sensor demonstrated a linear dynamic range of 0.7–14 μM (Fig.-2(d,e)) for both DA and UA, with detection limits of 0.6052 μM and 0.6462 μM, respectively. The linear regression equations for DA and UA demonstrated excellent linear relationships between current and concentration: I (μA) = 5.8156 cDA (μM) + 5.869 (R^2 = 0.9981) and I (μA) = 5.6964 cUA (μM) + 6.3795 (R^2 = 0.9979). Comparative evaluation with various electrochemical sensors, as reported in Table-1, indicates that the AuNPs/PM/CPE sensor exhibits superior analytical performance, as evidenced by its broader linear range and lower detection limits for the simultaneous analysis of DA and UA. These findings demonstrate that modification of the CPE surface with PM and AuNPs significantly enhances sensitivity and electron-transfer efficiency. The AuNPs/PM/CPE sensor therefore holds promise for highly accurate analysis of biological samples.

Table-1: Comparison of the Proposed AuNPs/PM/CPE Sensor with Previously Reported Electrochemical Sensors for the Simultaneous Determination of DA and UA

Sensor	Detection limit (mM)		Ref.
	DA	UA	
MOF-235/GCE	3.34	3.46	27
PEDOT-GO/GCE	2.0	10.0	28
Activated graphene-modified electrodes	1.96	1.97	16
PEDOT-GO	2.00	1.00	29
PdNPs/rGO/GCE	1.00	16.67	30
AuNPs/PM/CPE	0.60	0.64	This work

Reproducibility and Stability

The reproducibility and stability of the AuNPs/PM/CPE electrode were systematically evaluated by differential pulse voltammetry (DPV) for the simultaneous analysis of UA and DA. Measurements were performed in 0.1 M PBS (pH 3.0) with DA and UA concentrations of 20 μM and 70 μM, respectively. Reproducibility tests were carried out using five independently prepared modified electrodes. Each electrode was used to measure the peak current response of both analytes, and the results were compared to assess the consistency and analytical reliability of the developed electrode system. The relative standard deviation (RSD) values were 1.18% for DA and 3.73% for UA, indicating excellent reproducibility. For repeatability evaluation, 25 consecutive measurements were performed using a single modified electrode under identical experimental conditions. The resulting anodic peak currents gave RSD values of 0.81% for DA and 1.31% for UA, confirming the high repeatability and operational stability of the proposed sensor.

To further assess the practical applicability of the sensor, its selectivity was evaluated in the presence of potential interfering compounds**.** The voltammetric response was investigated using a mixed solution containing 1 μM each of DA, UA, and AA in 0.1 M PBS (pH 6.5) by DPV. The resulting voltammograms exhibited three well-defined oxidation peaks corresponding to DA, UA, and AA (Fig.-2(f)). The clear peak separation demonstrates that the AuNPs/PM/CPE electrode possesses excellent selectivity, enabling the simultaneous determination of all three analytes with minimal mutual interference.

The excellent reproducibility, repeatability, and selectivity obtained in this study demonstrate the effectiveness of the dual modification strategy using polymelamine and gold nanoparticles**.** The synergistic combination of these materials enhances electron-transfer efficiency, increases the electroactive surface area, and improves catalytic activity, resulting in reliable electrochemical performance for the simultaneous determination of UA and DA. Furthermore, the use of inexpensive materials and a straightforward fabrication procedure makes the proposed sensor attractive for practical biomedical applications. These characteristics support the development of accessible electrochemical

diagnostic technologies and are consistent with Sustainable Development Goal (SDG) 3 (Good Health and Well-Being), which promotes improved healthcare through innovative diagnostic tools.

Real Biological Sample Analysis

Simultaneous determination of UA and DA in urine samples was performed using the standard addition method to improve analytical accuracy and minimize matrix interference in complex biological systems. The urine samples were first diluted 50-fold with 0.1 M PBS (pH 3.0) as the supporting electrolyte. Subsequently, UA and DA standard solutions were added to achieve final concentrations of 1 μM each. Measurements were performed using the DPV technique, and the analytical results are presented in Table-2. The recovery values obtained were 98.99% for DA and 98.96% for UA, demonstrating the excellent accuracy and reliability of the proposed sensor for the analysis of real biological samples.

Table-2: Recovery Study of DA and UA in Human Urine Samples

Sample	Analyte	Added Concentration (μM)	Found Concentration (μM)	Recovery (%)
Urine	DA	0	ND	-
		1	0.9899	98.99
	UA	0	ND	-
		1	0.9896	98.96

CONCLUSION

A simple and effective AuNPs/PM/CPE working electrode was successfully developed for the simultaneous analysis of UA and DA. The electrode modification resulted in enhanced electrocatalytic activity, improved current response, and well-defined oxidation peaks for both UA and DA. The developed **electrode** also demonstrated high stability, reproducibility, and excellent selectivity in the presence of AA. The sensor was successfully applied to the simultaneous determination of DA and UA in human urine samples, achieving recoveries of 98.99% for DA and 98.96% for UA. This research also contributes to Sustainable Development Goal (SDG) 3 (Good Health and Well-Being), as the developed sensor shows considerable potential for the early detection of abnormal UA and DA levels.

ACKNOWLEDGMENTS

The authors gratefully acknowledge the financial support provided by the Indonesia Endowment Fund for Education (LPDP) through the Education Scholarship Program, administered by the Center for Higher Education Funding and Assessment, Ministry of Higher Education, Science, and Technology, Republic of Indonesia.

CONFLICT OF INTERESTS

The authors declare that there is no conflict of interest.

AUTHOR CONTRIBUTIONS

The present work is related to *SDG-3: Good Health and Well-Being.* All the authors contributed significantly to this manuscript, participated in reviewing/editing and approved the final draft for publication. The research profile of the authors can be verified from their ORCID ids, given below:

Erna Fitriany https://orcid.org/0000-0001-8532-2049
Muji Harsini https://orcid.org/0000-0001-5195-5665
Fredy Kurniawan https://orcid.org/0000-0003-2720-8314
B.A.Widyaningrum https://orcid.org/0000-0001-8811-072X
D.R.A. Paramita https://orcid.org/0000-0002-8817-9433

Cite this article as: E. Fitriany *et al.*, *Rasayan J. Chem.*, 19(3), 1683-1691(2026), https://doi.org/10.31788/RJC.2026.1939663

REFERENCES

1. G.S. Geleta, *Sensing and Bio-Sensing Research*, **43**, 100610(2024), https://doi.org/10.1016/j.sbsr.2023.100610
2. P.M. Moran and K.T. Granger, *Pharmacological Research*, **216**, 107727(2025), https://doi.org/10.1016/j.phrs.2025.107727
3. R. Mondal, N. Mukherjee and Sk.F. Ahmed, *Inorganic Chemistry Communications*, **178(1)**, 114449(2025), https://doi.org/10.1016/j.inoche.2025.114449
4. M.O. Klein, D.S. Batagello, A.R. Cardoso, D.N. Hauser, J.C. Bittencourt and R.G. Correa, *Cellular and Molecular Neurobiology*, **39(1)**, 31(2019), https://doi.org/10.1007/s10571-018-0632-3
5. Y. Vadivelu, A. Sendrayal Raj, R. Muniyandi, S.R. Srither and B. Ramachandran, *Talanta Open*, **12**, 100477(2025), https://doi.org/10.1016/j.talo.2025.100477
6. M. Harsini, B.A. Widyaningrum, D. Suryaningrum, S. Paramesti, A. Baktir, G. Pari and F.D. Priyani, *Rasayan Journal of Chemistry*, **17(3)**, 1377(2024), https://doi.org/10.31788/RJC.2024.1738850
7. M. Harsini, A.N. Farida, E. Fitriany, D.R.A. Paramita, A. Baktir, F. Kurniawan, S.C.W. Sakti, Y.D. Kurniawan and B.A. Widyaningrum, *Indonesian Journal of Chemistry*, **24(1)**, 38(2024), https://doi.org/10.22146/ijc.83301
8. M. Harsini, B.A. Widyaningrum, E. Fitriany, D.R.A. Paramita, A.N. Farida, A. Baktir, F. Kurniawan, S.C.W. Sakti and Y.D. Kurniawan, *Chinese Journal of Analytical Chemistry*, **50(4)**, 100052(2022), https://doi.org/10.1016/j.cjac.2022.100052
9. B. Tutunaru, *International Journal of Electrochemical Science*, **19**, 100493(2024), https://doi.org/10.1016/j.ijoes.2024.100493
10. E.D. Koshevaya, D.D. Maslov, E.M. Shishmakova, V.I. Mikhaylov, A.V. Belousov, O.Yu. Grafov, I.A. Novakov and A.V. Sysoev, *Colloids and Surfaces A: Physicochemical and Engineering Aspects*, **732**, 139147(2026), https://doi.org/10.1016/j.colsurfa.2025.139147.
11. J.B.M. Parambath, K. Vijai Anand, I.M. Ahmady, K. Hasan, H. Alawadhi, H. Lee, M. Al-Maadeed and S. Thomas, *Inorganic Chemistry*, **64(5)**, 4555(2025), https://doi.org/10.1021/acs.inorgchem.4c05588
12. P. Kanagavalli and S. Eissa, *Biosensors and Bioelectronics*, **259**, 116388(2024), https://doi.org/10.1016/j.bios.2024.116388
13. A. Bano, A. Dawood, Rida, F. Saira, A. Malik, M. Alkholief, H. Ahmad, M.A. Khan, Z. Ahmad and O. Bazighifan, *Scientific Reports,* **13**,12359(2023),https://doi.org/10.1038/s41598-023-38234-2
14. J. Hou, J.A. Lartey, C.Y. Lee and J.H. Kim, *Scientific Reports*, **14**, 1505(2024), https://doi.org/10.1038/s41598-024-51695-3
15. C. Liang, J.Y. Cheong, G. Sitaru, S. Rosenfeldt, A.S. Schenk, S. Gekle, F. Faupel and A.R. Boccaccini, *Advanced Materials Interfaces*, **9(4)**, 2100867(2022), https://doi.org/10.1002/admi.202100867
16. D. Li, M. Liu, Y. Zhan, Q. Su, Y. Zhang and D. Zhang, Microchimica Acta, 187, 94(2020), https://doi.org/10.1007/s00604-019-4083-4.
17. N. Mathur, K. Pachar, Ankita, A. Yadav, P. Roy and P. Gupta, *Electrochimica Acta*, **539**, 147131(2025), https://doi.org/10.1016/j.electacta.2025.147131
18. J. Barrio and A. Thomas, *Advanced Science*, **12(40)**, 2510137(2025), https://doi.org/10.1002/advs.202510137
19. Y. Lyu, L.M. Becerril, M. Vanzan, S. Corni, M. Cattelan, G. Granozzi, M. Prato and S. Agnoli, *Advanced Materials*, **36(10)**, 2211624(2024), https://doi.org/10.1002/adma.202211624.
20. W. Wang, D. Wang, H. Song, D. Hao, B. Xu, J. Ren, Y. Wang and H. Zhang, *Chemical Engineering Journal*, **455**, 140909(2023), https://doi.org/10.1016/j.cej.2022.140909.
21. X. Chen, Y. Wu, Y. Qin, R. Carmieli, I. Popov, V. Gutkin, Y. Rosenwaks and E. Joselevich, *ACS Nano*, **19**, 9981(2025), https://doi.org/10.1021/acsnano.4c16272.
22. M.P. Pinz, I. Medeiros, L.A. da C. Carvalho and F.C. Meotti, *Redox Report*, **30(1)**, 2498105(2025), https://doi.org/10.1080/13510002.2025.2498105.

23. H. Muhammad, I.A. Tahiri, M. Muhammad, Z. Masood, M.A. Versiani, O. Khaliq, M.A. Sheikh, M.A. Tahir and M.I. Bhanger, *Journal of Electroanalytical Chemistry*, **775**, 157(2016), https://doi.org/10.1016/j.jelechem.2016.05.049.
24. A. P. F. Turner, *Chemical Society Reviews*, **42(8)**, 3184(2013), https://doi.org/10.1039/C3CS35528D
25. F.J. Priya, A.L. Rose, S. Vidhya, A. Arputharaj and A. Revathii, *Rasayan Journal of Chemistry*, **18(2)**, 1200(2025), https://doi.org/10.31788/RJC.2025.1829227
26. G.C. Paul, S. Bhowmik, J. Biswas, S. Bhowmik and U. Majumder, *Rasayan Journal of Chemistry*, **19(1)**, 133(2026), https://doi.org/10.31788/RJC.2026.1919469.
27. K. Liu, Y. Chen, X. Dong and H. Huang, *Inorganic Chemistry Communications*, **142**, 109584(2022), https://doi.org/10.1016/j.inoche.2022.109584.
28. D. Li, M. Liu, Y. Zhan, Q. Su, Y. Zhang and D. Zhang, *Microchimica Acta*, **187**, 94(2020), https://doi.org/10.1007/s00604-019-4083-4.
29. S.H. Ko, S.W. Kim and Y.J. Lee, *Scientific Reports*, **11**, 21056(2021), https://doi.org/10.1038/s41598-021-00712-w.
30. Y. Wei, Y. Liu, Z. Xu, S. Wang, B. Chen, D. Zhang, X. Wang and Y. Zhang, *International Journal of Analytical Chemistry*, **2020**, 8812443(2020), https://doi.org/10.1155/2020/8812443.

[RJC-9663/2026]